

# LoRa-E: Overview and Performance Analysis

Guillem Boquet, Pere Tuset-Peiró, *Senior Member, IEEE*, Ferran Adelantado, *Senior Member, IEEE*, Thomas Watteyne, *Senior Member, IEEE*, Xavier Vilajosana, *Senior Member, IEEE*

**Abstract**—LoRa-E is a new physical layer developed by Semtech to increase the capacity of LoRaWAN in dense and congested deployments. It has also been designed to address extremely long-range and large-scale communication scenarios with a focus on reaching gateway devices installed on satellites. Thanks to its design principles, it finely manages packet transmission, enabling Quality-of-Service policies on a per-packet basis. The core of LoRa-E is a Fast Frequency Hopping Spread Spectrum Modulation (FHSS) that uses frequency hopping sequences in which  $\sim 50$  ms fragments are transmitted. Given the notorious adoption of LoRaWAN in the IoT application landscape, this article is a reference for understanding how exactly LoRa-E works, what performance it offers, and what its limitations are.

**Index Terms**—LoRaWAN, LoRa-E, Limits, LPWAN, Satellite Networks

## I. INTRODUCTION

The Internet of Things (IoT) relies on low-power wireless communication technologies and protocols to enable reliable wireless communication between distributed sensor and actuator devices. Over the last decade, we have seen the rise of Low-Power Wide Area Network (LPWAN) technologies [1], with LoRaWAN becoming one of the most prominent players in the market thanks to long-range and robust communication, coupled with a simple network architecture that allows for solutions that are easy to deploy and manage. At the physical layer, LoRaWAN uses Long Range (LoRa), a robust Chirp Spread Spectrum (CSS) modulation developed by Cycleo, later acquired and commercialized by Semtech under the LoRa trademark. The LoRa physical layer is designed to prioritize uplink communication and ensure low power operation, limited by a low data rate (250 bps with spreading factor 12 and 125 kHz channel as the most restrictive) and kilometer-scale communication range. Different configurations of the physical layer are available –referred to as Data Rates (DR)– providing different levels of chirp redundancy and thus trading off bandwidth utilization and robustness. LoRaWAN defines different bandwidth configurations per channel, ranging from 125 kHz to 500 kHz, depending on the regional parameters and available bandwidth. The access to these channels is based on pure ALOHA, limited by regional duty cycle regulations which constrain the time-on-air that can be utilized per device, further limiting the maximum achievable throughput [2].

The technology has been widely adopted. However, there are drawbacks and limitations to LoRaWAN, particularly in dense deployments where performance, that is, the overall

This project is co-financed by the EU Regional Development Fund within the ERDF Operational Program of Catalonia 2014-2020 with a grant of 50% of total cost eligible, the SPOTS project (RTI2018-095438-A-I00) funded by the Spanish Ministry of Science, and the 2017 SGR 60 by the Generalitat de Catalunya.

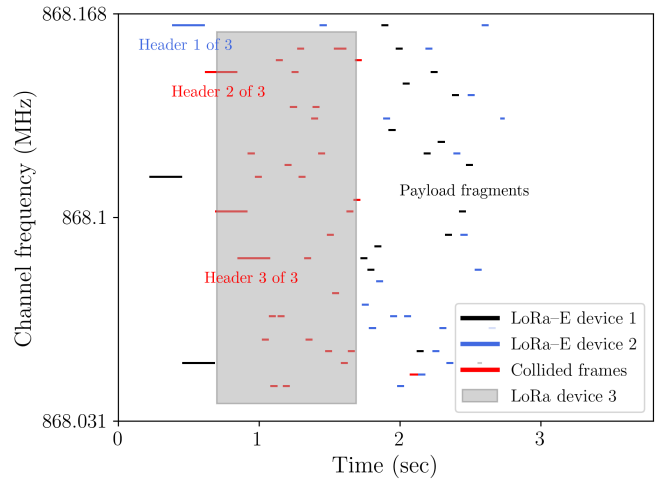


Fig. 1. Two LoRa-E (DR8 mode) 30-byte and one LoRa (DR0/SF12) 10-byte packets transmitted simultaneously in the EU 868-870 MHz band (Channel 1, 137 kHz bandwidth, 868.031 to 868.168 MHz). Despite several frame collisions, both LoRa-E packets will be decoded successfully with high probability thanks to FHSS and coding redundancy.

network capacity, is severely limited by duty-cycle regulations and the use of simple Medium Access Control (MAC) protocols [3]. In that sense, the research community has issued during the last years several proposals to address the fundamental operation of LoRaWAN at the physical and data-link layers [4], [5], as well as the overall system operation [6], using both analytic models and simulations [7]. In addition, the scalability and reliability issues of LoRaWAN have been the focus of recent research efforts towards ensuring fairness [8], improving channel usage [9], or even scheduling LoRa transmissions [10].

As a novelty, Semtech has announced an extension of the LoRa physical layer called “LoRa-E” [11]. The extension is motivated by emerging use cases with increasingly larger and denser network deployments, including satellite-scale LoRaWAN networks. Its main goal is to increase network capacity and robustness by adopting the basis of frequency hopping modulation, while keeping the same communication range than LoRa and meeting ETSI [12], FCC [13] and ARIB [14] regulations. Additionally, LoRa-E has been designed to introduce higher levels of network flexibility, targeting applications that require differentiated service levels.

We expect LoRa-E to have a big impact on LPWAN and enable viable satellite IoT solutions. Therefore, in this article, we provide an overview of the technology and its performance, comparing it to today’s LoRa, and validate the scalability gain announced by Semtech. We also identify open research

issues and directions for this new physical layer. To that aim, the remainder of this article is organized as follows. Section II presents an overview of LoRa-E. Section III studies the scalability of LoRa-E networks and compares it to LoRa networks. Section IV outlines open research questions for LoRa-E networks. Finally, Section V concludes the article.

## II. LORA-E OPERATION

As most LPWANs, LoRaWAN prioritizes uplink capacity and limits downlink transmissions to sporadic data or control packets. LoRa-E is a fast Frequency Hopping Spread Spectrum (FHSS) modulation used only for uplink. It relies on two different bit rates (162 bps and 325 bps) according to the novel data rate (DR) modes explained in Section II-A. Downlink communication is achieved with the current LoRa modulation, since the same radios can switch between modulations.

To initiate transmission of a LoRa-E packet (Section II-B), the end-device randomly selects one of the LoRa-E channels available and uses a pure ALOHA access mechanism. As illustrated in Fig. 1, those channels are divided into several sub-channels (Section II-C) that are used for frequency hopping. First, a number of replicas of the same header are transmitted in the selected channel following the device's channel hopping sequence. The number of replicas is defined by each LoRa-E data rate mode. After the packet headers are transmitted, the packet payload is split into fragments with a duration of  $\sim 50$  ms, which are sent consecutively in each sub-channel determined by the hopping sequence (Section II-D). Contrary to the packet header, only a single copy of each fragment is transmitted. At the other end, the gateway reassembles the packet payload using the information within a header.

Unlike for LoRa channels, as long as the LoRa-E transmissions fall entirely in the gateway processed LoRa-E bandwidth, the packets can be demodulated. This means that the gateway does not need to know in advance any channel hopping sequences, nor the exact channels frequencies and bandwidths. Therefore, different devices can use a different spreading bandwidth and may not all have the channel at the same frequency. It also implies that multiple transmitters can operate at the same time, provided they use different channel hopping sequences and the gateway is able to listen to the whole channel bandwidth at the same time. This increases the complexity of signal detection at the receiver, compared to LoRa. However, it allows hundreds of packets to be received simultaneously, which is appropriate for satellite-scale networks where the number of devices interfering within the coverage area of a gateway located at space is much greater than the number of devices found in current LoRaWAN use cases.

LoRa-E can be used with limited support (no intra-packet hopping) for current SX1272/76 devices through a firmware update. In contrast, the newer SX1261, SX1262 and SX1268 modems are fully LoRa-E compatible and can take advantage of its frequency hopping modulation technique. Lastly, demodulation can be achieved by all V2 gateways by firmware upgrade.

### A. LoRa-E Data Rates

LoRa-E modes are organized into different data rates, shown in Table I. DR0-DR4 correspond to SF12-SF8 in today's LoRaWAN. In the EU863-870 band, those are DR8/DR10 (slower, higher robustness) and DR9/DR11 (faster, lower robustness). DR8 and DR10 use a coding rate of  $1/3$ , 3 header repetitions, and a physical bit rate of 162 bps. DR9 and DR11 use a coding rate of  $2/3$ , 2 header repetitions, and a physical bit rate of 325 bps. The aforementioned coding rates are used to convolutionally encode the payload bits that are decoded using Viterbi algorithm, providing maximum likelihood performance. Although the specification allows for header repetitions ranging from 1 to 4, only the two configurations above are used. This redundancy is key to ensuring the robustness of LoRa-E when fragments are spread in frequency. For example, the gateway device is able to reassemble a packet transmitted using DR9 with high probability even if 1 of the 2 headers and  $1/3$  of the bits within the payload fragments are lost. These mechanisms mitigate the impact of interference from other LoRa and LoRa-E devices operating in the same band, as well as devices using other wireless technologies.

### B. LoRa-E Packet Format

As shown in Fig. 2, a LoRa-E packet is composed of a SyncWord, a PHY Header (which includes a CRC) and the payload (which also includes a CRC). The first transmitted fragments (2 or 3 replicas) contain the entire header (SyncWord, Header, Header CRC). The header is transmitted at a fixed bit rate for a duration of 0.233 s, containing information about channel hopping sequence, payload length, data rate, number of header replicas and coding rate. Note in Fig. 1 the transmission of 3 consecutive header replicas with the same duration, which are not split across multiple fragments despite being longer than  $\sim 50$  ms. Each packet header contains the necessary information such that the gateway can compute the exact list of frequencies that the packet will be using. Thus, the gateway must receive at least one copy of the header to be able to detect and reassemble the packet. Moreover, LoRa-E enables to trim on a packet per packet modulation density (GMSK, QPSK, 16QAM), number of header repetition, coding rate and frequency spreading bandwidth, allowing flexible fine grained network resource management to reach the required QoS for each device individually, as it can reserve less occupied spectrum for high QoS/weak devices. The next fragments (Fig. 1) only contain the payload and are transmitted at the configured data rate with a fixed duration of  $\sim 50$  m each. Recall that its information is encoded in the fragments in such a way that even if  $1/3$  of the fragments are lost, the information can still be recovered and the packet reassembled with high probability.

### C. LoRa-E Channels and Sub-Carriers

Similar to LoRaWAN, the frequency band is split into different Operating Channel Width (OCW) channels. The number of channels available depends on the region of the world in which the network operates, thus white-list is used to mark those

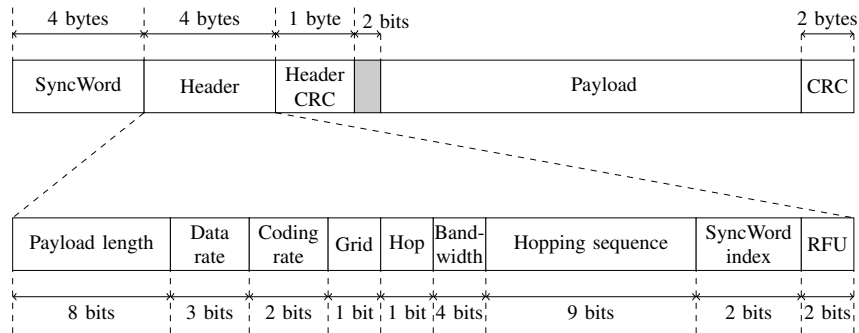


Fig. 2. LoRa-E packet structure. While the header 5 bytes long (including Header-CRC), the radio transmits 80 bits as it is using a convolutional code with coding rate  $1/2$ . Between the header and the payload, the transceiver waits for a time equivalent to 2 bits (shaded gray) to allow the receiver to decode and process the header. The header is 114 bits long, the payload can be up to 125 bytes long.

channels. In North America (FCC 902-928 MHz), the specification defines 8 LoRa-E OCW channels with 1.523 MHz bandwidth and center frequencies equal to  $(903 + 1.6n)$  MHz,  $n = 0, \dots, 7$ . In Europe (ETSI 863-870 MHz), the LoRa-E OCW channels are defined to have a bandwidth equal to 137 kHz or 336 kHz depending on the selected data rate mode. The number of channels that can be used depends on the specific gateway technology used by the network operator. The number of LoRa-E channels supported by a gateway depends on the number of Digital Signal Processors (DSPs) used; each DSP covering 1.523 MHz. For example, in a gateway with one DSP and 200 kHz channel spacing, end-devices can use up to 7 LoRa-E channels when using a 137 kHz OCW channel for the uplink.

Each LoRa-E OCW channel is divided into several Occupied Band Width (OBW) physical channel sub-carriers with a bandwidth of 488 Hz. For example, the 137 kHz channel bandwidth in the EU 863-870 MHz regional parameters enables 280 LoRa-E OBW sub-carriers in a single LoRa-E OCW channel, therefore supporting simultaneous transmission. Because the regional regulations impose restrictions on the time and bandwidth occupation, sub-carrier hopping policies must have a minimum frequency hop. That is, two consecutive sub-carriers of a hopping sequence must be separated by a minimum distance. In the EU band, the minimum frequency shift is 3.9 kHz for each fragment [12], thus creating 8 simultaneous grids of 35 usable sub-carriers in each of the 137 kHz LoRa-E OCW channels in DR8/DR9. In the US band, the minimum separation between LoRa-E hopping sub-carriers is 25.4 kHz. Similarly, this requirement results in 52 simultaneous groups of 60 usable sub-carriers for each particular 1.523 MHz OCW channel.

Table I summarizes the LoRa-E physical layer both for ETSI and FCC regulations. In some configurations, the relatively small number of sub-carriers in a group (e.g. 35 sub-carriers in each of the 8 groups in an EU 137 kHz OCW channel) may cause fragment collisions, as these are sent in a pseudo-random frequency hopping pattern. However, the probability of concurrent transmissions, that is, two end devices selecting the same frequency hopping pattern at approximately the same time, is very low.

#### D. Frequency Hopping Policy

For each uplink packet, the device randomly selects a channel amongst the ones enabled that can support the data rate. The transmission starts on a random physical sub-channel (grid) inside the LoRa-E spreading bandwidth, then follows a pseudo-random frequency hopping pattern computed by the device. Given a specific OCW frequency offset, the hopping pattern is obtained as the outcome of a simple 32-bit hash function executed by the LoRa-E device, modulo the number of available channels in the grid or physical sub-carriers usable for channel hopping per end-device transmission (35 or 86 in EU and 60 in USA, Table I). In particular, the input of the hash function is determined by the result of a device-specific 9-bit random number (set at the Hopping Sequence field in the header, Fig. 2) plus the product of the current fragment number and  $2^{16}$ . Finally, the hash is multiplied by the minimum frequency separation between LoRa-E hopping carriers to comply with the regulations of the transmission band. All of this ensures a pseudo-random pattern where all physical channels are statistically used equally.

### III. KEY PERFORMANCE ASPECTS

Understanding the performance of LoRa-E under saturation conditions and how it compares to LoRa are essential questions to any LoRa-E prospective user. In this section, we evaluate and compare its performance from the end-device and the network scalability perspective.

To evaluate its key performance aspects we have developed a packet-based network simulator that implements the basic functionality of both protocols<sup>1</sup>. The simulator uses an exponential distribution to model the random time between independent packet arrivals, where the arrival rate is established at the maximum transmission rate allowed by the duty cycle regulations. Packets are allocated in a discrete time and frequency space with a millisecond time resolution and OBW sub-carrier granularity. Simultaneous transmissions only cause a collision if they both select the same OBW sub-carrier and overlap in time. For each LoRa-E device, a channel

<sup>1</sup>As an online addition to this article, the source code of the simulator is published under an open-source license at [LINK TO BE ADDED AFTER PAPER IS ACCEPTED](#).

Region	European Union (ETSI, 863-870 MHz)				United States (FCC, 902-928 MHz)	
LoRa DataRate Alias	DR8	DR9	DR10	DR11	DR5	DR6
LoRa-E Num Channels	7	4	7	4	8	
LoRa-E OCW (kHz)	137		336		1523	
LoRa-E OBW (Hz)	488					
Minimum separation between LoRa-E hopping carriers (kHz)	3.9				25.4	
Number of physical carriers available for frequency hopping in each OCW channel	280 (8x35)		688 (8x86)		3120 (52x60)	
Number of physical carriers usable for frequency hopping per end-device transmission	35		86		60	
Coding Rate	1/3	2/3	1/3	2/3	1/3	2/3
Physical bit rate (bits/s)	162	325	162	325	162	325
Max. MAC Payload Size (bytes)	58	123	58	123	125	125
Max. MAC Payload Fragments	61	64	61	64	130	65
Header replicas	3	2	3	2	3	2
PHY Header duration per replica (seconds)	0.233	0.233	0.233	0.233	0.233	0.233
PHY Time on Air (seconds)	0.70 + 3.06	0.47 + 3.19	0.70 + 3.06	0.47 + 3.19	0.70 + 6.48	0.47 + 3.24

TABLE I

LoRa-E MAIN SPECIFICATIONS AND PARAMETERS FOR EU (ETSI, 868-870 MHz) AND US (FCC, 902-928 MHz) REGIONS.

hopping sequence is created at the beginning, according to the procedure described in Section II and the parameters presented in Table I. That is, LoRa-E packets are divided into several fragments and spread following the device's hopping sequence at transmission time. At reception, a LoRa-E packet is successfully decoded if minimum one of the headers and 1/3 (or 2/3) of the payload have not collided. For LoRa, packets are transmitted using the entire available channel bandwidth, and decoded only if they have not collided.

We perform an extensive simulations campaign assuming the EU 863-870 MHz band, which imposes the most restrictive per-channel duty cycle of 1%. Simulations are conducted assuming ideal end-device and channel conditions. Therefore, the results shown below should be considered as a lower bound of the expected performance of both LoRa and LoRa-E. We do *not* model crystal drift, which would cause the frequency grids of different end-devices to be slightly offset. However, the impact of these effects in the network performance is negligible considering the randomness of frequency hopping patterns and the robustness of the LoRa-E modulation.

#### A. LoRa-E End-device Capacity

Fig. 3 shows the time-on-air (*top*) and the number of packets per hour per end-device (*bottom*) for different MAC payload sizes (10 B, 50 B) for LoRa DR0 (SF12), DR5 (SF7 125 kHz), and the LoRa-E data rates available in Europe (DR8/10 and DR9/11). As depicted, LoRa DR5 provides the highest number of packets per hour per end-device (369.1 to 873.5), whereas LoRa-E DR8/10 provides the least (10.7 to 27.5). In contrast, LoRa DR0 provides between 15.6 and 36.3 packets per hour per end-device, whereas LoRa-E DR9/11 provides similar capacity regardless of the MAC payload size, having between 20.1 and 46.6 packets per hour per end-device.

As expected, the lower LoRa-E datarate combined with the imposed duty cycle regulations limit the number of packets that can be transmitted. Observing these results, one could conclude that using LoRa-E does not provide any real benefit in terms of individual end-device capacity. However, LoRa-E is not designed to increase the number of packets that can be transmitted by each end-device independently. Rather,

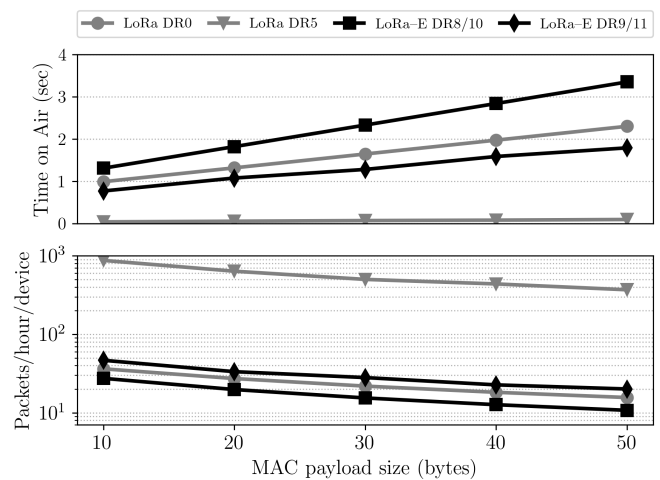


Fig. 3. Relationship between the packet duration (seconds) and the maximum per end-device transmission rate (packets/hour) when abiding to the EU 868-870 MHz band regulation, which imposes a 1% duty cycle per device and channel.

the strength of LoRa-E lays in the overall network capacity increase provided by the statistical multiplexing of combining time and frequency diversity.

#### B. LoRa-E Network Capacity

Fig. 4 compares a 125 kHz LoRa channel with a 137 kHz LoRa-E channel (supporting 8 grids of 35 physical sub-carriers), and shows how LoRa-E scales with the number of end-devices transmitting at the maximum possible rate using a payload of 10 B. As it can be observed, the number of supported end-devices peaks at 50 when using LoRa regardless of the DR used. This can be explained by the fact that the network is limited at the data-link layer by the ALOHA MAC protocol, and at the physical layer by the radio duty cycle regulation (1% at the EU 868-870 MHz band). Higher DRs provide higher goodput because each DR (almost) doubles the data rate of the previous one, hence the transmission time on air of the packet decreases proportionally and more

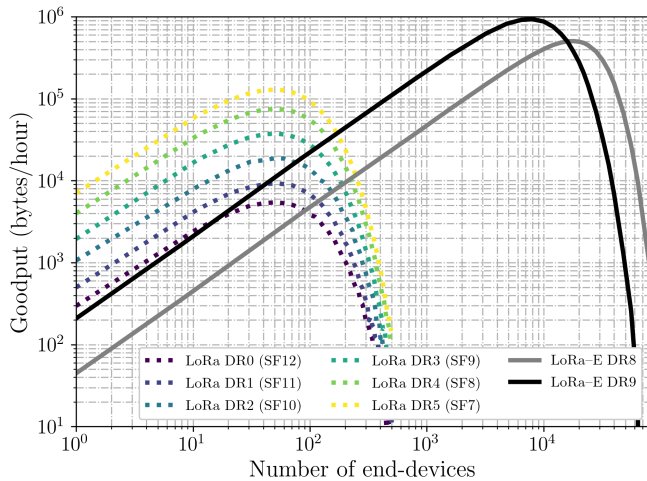


Fig. 4. Total useful bytes received per hour (goodput) when a given number of LoRa and LoRa-E end-devices transmit 10 B of payload at the maximum 1% duty cycle allowed by the EU 868-870 MHz regulation. Both LoRa and LoRa-E results are obtained considering 125 kHz and 137 kHz channels, respectively.

packets (information) can be fitted, offering the same channel load. In other words, the total offered load remains constant despite the DR used because devices' maximum transmission rate is fixed by the duty-cycle regulation, that is, a higher DR provides additional capacity, resulting in an unchanged collision probability in this scenario. Simulations performed with payload sizes up to 50 B showed the same behavior.

In contrast, thanks to the OCW sub-carrier spreading in LoRa-E, the number of end-devices that can transmit simultaneously increases, leading to a significant increase in the goodput of the entire network as it scales. Notably, LoRa-E ensures a goodput proportional to the throughput that is one order of magnitude larger than LoRa for the fastest of the DRs (DR5) and two orders of magnitude for the slowest (DR0). The maximum goodput while using DR9/DR8 and a payload size of 10 B occurs when 8,000/18,000 end-devices transmit at the maximum allowed rate (given the payload size, Fig. 3) or, in other words, 370,000/500,000 packets with 10-B payload are generated per hour within the network. Above that number of end-devices or generated packets per hour, the performance of DR9 decreases faster than DR8, causing DR8 to scale better. This is because DR8 repeats the header 3 times (2 times in DR9) and transmits more redundant information for error correction (i.e., coding redundancy 1/3 in DR8, 2/3 in DR9) which increases robustness against collisions. Thus, we can extrapolate that DR8 performs better than DR9 in terms of goodput on channels with significant interference. For example, in Fig. 4 when 16,000 or more end-devices are transmitting simultaneously at the maximum allowed rate, the LoRa-E DR8 network outperforms DR9.

Fig. 5 shows the crossover points between LoRa and LoRa-E goodput as a function of the number of generated packets per hour for the different LoRa DR configurations and MAC payload sizes (i.e., 10 B and 50 B). If we compare LoRa-E with devices transmitting 10 B of payload size against

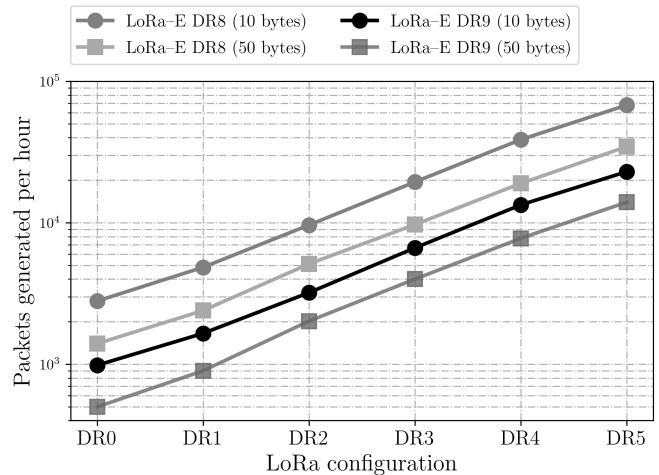


Fig. 5. Comparison between LoRa and LoRa-E DRs performance. Markers show the crossover points in number of generated packets per hour required for LoRa-E to provide a better goodput than LoRa, as a function of payload size.

the lowest LoRa data rate configuration (DR0), the LoRa-E network requires a network load greater than 2,800 and 985 packets/hour for DR8 and DR9, respectively, to provide a higher goodput than the LoRa DR0 network. At the other end, LoRa-E requires around 68,000 packets/hour for DR8 and 23,000 packets/hour for DR9 to provide higher goodput compared to the LoRa DR5 configuration. This is an exponential growth with a growth rate of almost 2, similar to the increase in the available data rate when the LoRa DR is increased from DR0 to DR5. The same growth rate is found when devices transmit 50 B of payload size. However, the crossover points occur for lower values of generated packets per hour, meaning that LoRa-E is more efficient in terms of goodput when the ratio between payload and overhead increases. Interestingly, the required number of packets/hour needed for LoRa-E to be greater than LoRa is divided by 2 if devices increase the payload size from 10 to 50-B. For example, regarding LoRa-E DR8 and LoRa DR0, the crossover point for 10 B is at 2,800 packets/hour while for 50 B is at 1,400 packets/hour.

Finally, notice that the results presented are for a single LoRa and LoRa-E channel and, hence, the overall network capacity has to be multiplied by the number of available channels and DR configurations in the band of interest. For example, transmitting a 10-B payload in the EU 868-870 MHz band, a legacy LoRa DR0 network could ideally support a total load of 96,000 packets/hour at its peak efficiency, when considering the use of 8 independent 125 kHz channels and 6 DRs simultaneously. In contrast, the total capacity of a EU LoRa-E network would be around 3.5M packets/hour when using DR8, and 1.48M packets/hour when using DR9. This assumes 7 and 4 channels with 8 frequency grids each, as summarized in Table I, which represents a 36 $\times$  and 15 $\times$  capacity increase for LoRa-E when compared to LoRa.

### C. LoRa-E Use Case

With a lower data rate than DR0 (SF12), the time on air for a LoRa-E packet and the number of packets that an end-device can transmit during a period of time is smaller than LoRa. Yet, this nominal under-performance does not translate into an effective reduction of the goodput because fragment spreading reduces collision probability. This mode of operation can also be exploited to scale the network in terms of the number of end-devices supported concurrently. That is, LoRa-E slices the spectrum so that multiple end-devices can use the same channel with a insignificantly low collision probability. Hence, LoRa-E offers higher network scalability when compared to LoRa DR0.

Considering the presented results, we can conclude that LoRa-E provides better network scalability than LoRa thanks to the adoption of FHSS modulation technique. In particular, the 162 bps LoRa-E data rate provides two orders of magnitude more network capacity, while offering the same radio link budget than LoRa DR0 (SF12). In addition, LoRa-E retains the long-range communication characteristics of LoRa. This makes LoRa-E suitable for terrestrial and satellite deployments, where a high end-device density or a large gateway coverage area leads to an increased level of interference. Summarizing, LoRa-E allows the necessary  $>155$  dB link margin for LEO satellite IoT plus the capacity to receive hundreds of packets simultaneously.

### IV. OPEN RESEARCH CHALLENGES

This section discusses two main open research challenges presented by LoRa-E: optimal selection of frequency hopping sequences and coexistence with legacy LoRa networks.

#### A. Optimal Frequency Hopping Sequences

The LoRa-E specification uses a simple frequency hopping pattern based on a 32-bit hash function. These hopping sequences create grids on the OCW channels that space sub-carriers a minimum frequency distance according to the region's specification. While these schemes ensure a spreading of the packets among the sub-carriers, optimal policies can be designed to address specific channel conditions. In particular, schemes that dynamically adapt sequences to continuously match a changing environment. Because LoRa-E networks can manage the spectrum used by each device individually, adaptive frequency hopping [15] can either aim to maintain data throughput or allow flexible fine-grained network resource management to achieve the desired QoS per device. Hence, an important research topic is to evaluate different hopping sequences and hash functions to maximize the properties of the FHSS scheme. Also, it would be interesting to explore sequence management policies that determine how and when these dynamic sequences need to be updated.

#### B. Coexistence with Legacy LoRa Networks

As LoRaWAN deployments will integrate end-devices using different LoRa DRs, including the novel LoRa-E, and will have to coexist with other LoRaWAN networks using

different combinations of DRs, coexistence is a key aspect to investigate. In particular, the results evaluating the coexistence between LoRa and LoRa-E DRs will allow to build recommendations and best-practice strategies for deploying these technologies and ensuring their performance. Such recommendations may be to dedicate some channels to LoRa-E, or to limit the proportion of different DRs in each channel. Another topic related to coexistence is Adaptive Data Rate (ADR), for which the role of LoRa-E needs to be defined. In that regard, LoRaWAN may have to include new functionalities to adapt to an increase in network load by dynamically switching to LoRa-E when the goodput degrades.

### V. CONCLUSIONS

LoRa-E has been recently released. LoRa-E's physical layer is designed to offer flexibility for differentiated services and increase the scalability of LoRaWAN networks, retaining its long-range communication characteristics. This article has presented LoRa-E, evaluated its performance and highlighted its limitations. Results show a significant increase in the scalability of the network at the cost of individual end-device capacity. This article has also discussed open research challenges to improve the performance of LoRa-E, including mechanisms to optimize the frequency hopping sequences, policies to properly plan and adapt the network to the load, as well as assessing the coexistence of LoRa with LoRa-E networks.

### REFERENCES

- [1] U. Raza, P. Kulkarni, and M. Sooriyabandara, "Low Power Wide Area Networks: An Overview," *IEEE Communications Surveys Tutorials*, vol. 19, no. 2, pp. 855–873, 2017.
- [2] F. Adelantado, X. Vilajosana, P. Tuset-Peiro, B. Martinez, J. Melia-Segui, and T. Watteyne, "Understanding the Limits of LoRaWAN," *IEEE Communications Magazine*, vol. 55, no. 9, pp. 34–40, 2017.
- [3] J. C. Liando, A. Gamage, A. W. Tengourtius, and M. Li, "Known and Unknown Facts of LoRa: Experiences from a Large-Scale Measurement Study," *ACM Trans. Sen. Netw.*, vol. 15, no. 2, Feb. 2019.
- [4] R. B. Sørensen, D. M. Kim, J. J. Nielsen, and P. Popovski, "Analysis of Latency and MAC-Layer Performance for Class A LoRaWAN," *IEEE Wireless Communications Letters*, vol. 6, no. 5, pp. 566–569, 2017.
- [5] D. Magrin, M. Capuzzo, and A. Zanella, "A Thorough Study of LoRaWAN Performance Under Different Parameter Settings," *IEEE Internet of Things Journal*, vol. 7, no. 1, pp. 116–127, 2020.
- [6] A. Mahmood, E. Sisinni, L. Guntupalli, R. Rondón, S. A. Hassan, and M. Gidlund, "Scalability Analysis of a LoRa Network Under Imperfect Orthogonality," *IEEE Transactions on Industrial Informatics*, vol. 15, no. 3, pp. 1425–1436, 2019.
- [7] F. Van den Abeele, J. Haxhibeqiri, I. Moerman, and J. Hoebeke, "Scalability Analysis of Large-Scale LoRaWAN Networks in ns-3," *IEEE Internet of Things Journal*, vol. 4, no. 6, pp. 2186–2198, 2017.
- [8] B. Reynders, W. Meert, and S. Pollin, "power and spreading factor control in low power wide area networks," in *2017 IEEE International Conference on Communications (ICC)*.
- [9] J. Ortín, M. Cesana, and A. Redondi, "Augmenting LoRaWAN Performance With Listen Before Talk," *IEEE Transactions on Wireless Communications*, vol. 18, no. 6, pp. 3113–3128, 2019.
- [10] B. Reynders, Q. Wang, P. Tuset-Peiró, X. Vilajosana, and S. Pollin, "Improving Reliability and Scalability of LoRaWANs Through Lightweight Scheduling," *IEEE Internet of Things Journal*, vol. 5, no. 3, pp. 1830–1842, 2018.
- [11] N. Sornin, M. Luis, T. Eirich, T. Kramp, and O. Hersent, "RP2-1.0.2 LoRaWAN Regional Parameters," *LoRa Alliance Technical Committee and others*, 2020.

- [12] E. T. ETSI, "Electromagnetic compatibility and Radio spectrum Matters (ERM); Short Range Devices (SRD); Radio equipment to be used in the 25 MHz to 1 000 MHz frequency range with power levels ranging up to 500 mW," *European harmonized standard EN*, vol. 300, no. 220, p. v3, 2019.
- [13] FCC, "FCC regulation. Title 47 Chapter I, Part 15, and Section 247: Operation within the bands 902-928 MHz, 2400-2483.5 MHz, and 5725-5850 MHz," *Federal Communications Commission (FCC)*, 2015.
- [14] ARIB, "920MHz-Band Telemeter, Telecontrol and Data Transmission Radio Equipment. Standard ARIB STD-T108," *Association of Radio Industries and Business*, p. v1.3, 2019.
- [15] P. Popovski, H. Yomo, and R. Prasad, "Strategies for adaptive frequency hopping in the unlicensed bands," *IEEE Wireless Communications*, vol. 13, no. 6, pp. 60–67, 2006.

**Guillem Boquet** received his M.Sc. and PhD. in Telecommunications Engineering from Universitat Autònoma de Barcelona (UAB) in 2014 and 2020 respectively. He is currently a Researcher at the WiNe (Wireless Networks) group of the Universitat Oberta de Catalunya (UOC).

**Pere Tuset-Peiró** (M'12, SM'18) is Assistant Professor at the Universitat Oberta de Catalunya (UOC) and Senior Researcher at the Wireless Networks (WiNe) group. He received his M.Sc. in Telecommunications Engineering from Universitat Politècnica de Catalunya (UPC), and his Ph.D. in Network and Information Technologies from Universitat Oberta de Catalunya (UOC).

**Ferran Adelantado** (M'08, SM'19) is Associate Professor at the Universitat Oberta de Catalunya (UOC) and Senior Researcher at the Wireless Networks (WiNe) group. He holds a M.Sc. degree in Telecommunications Engineering (2001) and a PhD (2007) from the Universitat Politècnica de Catalunya (UPC).

**Thomas Watteyne** (sM'06, M'09, SM'15) holds a PhD in Computer Science (2008), an MSc in Networking (2005) and an MEng in Telecommunications (2005) from INSA Lyon, France. He is a Research Director at Inria in Paris, leading the EVA research team, and network designer at Analog Devices. He previously worked at Orange Labs and UC Berkeley.

**Xavier Vilajosana** (M'09, SM'15) received his B.Sc. and M.Sc in Computer Science from Universitat Politècnica de Catalunya (UPC) and his Ph.D. in Computer Science from the Universitat Oberta de Catalunya (UOC). He has been a researcher at Orange Labs, HP and UC Berkeley. He is now Professor at the Universitat Oberta de Catalunya (UOC).